

# Closing in on the Fermi Line with a New Observation Strategy

Christoph Weniger,<sup>1</sup> Meng Su,<sup>2,3,4</sup> Douglas

P. Finkbeiner,<sup>2,5</sup> Torsten Bringmann,<sup>6</sup> and Nestor Mirabal<sup>7</sup>

<sup>1</sup>*GRAPPA Institute, Univ. of Amsterdam,*

*Science Park 904, 1098 GL Amsterdam, Netherlands*

<sup>2</sup>*Institute for Theory and Computation,*

*Harvard-Smithsonian Center for Astrophysics,*

*60 Garden Street, MS-51, Cambridge, MA 02138, USA*

<sup>3</sup>*Department of Physics, and Kavli Institute for Astrophysics and Space Research,  
Massachusetts Institute of Technology, Cambridge, MA 02139, USA*

<sup>4</sup>*Einstein Fellow*

<sup>5</sup>*Center for the Fundamental Laws of Nature, Physics Department,  
Harvard University, Cambridge, MA 02138, USA*

<sup>6</sup>*II. Institute for Theoretical Physics, University of Hamburg,  
Luruper Chaussee 149, 22761 Hamburg, Germany*

<sup>7</sup>*Universidad Complutense de Madrid, Spain*

Evidence for a spectral line in the inner Galaxy has caused a great deal of excitement over the last year, mainly because of its interpretation as a possible dark matter signal. The observation has raised important questions about statistics and suspicions about systematics, especially in photons from the Earth limb. With enough additional data, we can address these concerns. In this white paper, we summarize the current observational situation and project future sensitivities, finding that the status quo is dangerously close to leaving the issue unresolved until 2015. We advocate a change in survey strategy that more than doubles the data rate in the inner Galaxy, and is relatively non-disruptive to other survey science. This strategy will clearly separate the null hypothesis from the line signal hypothesis and provide ample limb data for systematics checks by the end of the extended survey. The standard survey mode may not.

## I. INTRODUCTION

For indirect dark matter searches with gamma rays, discriminating between a signal from conventional astrophysical backgrounds is challenging (for a recent review see [1]). Among various possible signatures, gamma-ray line emission is a long-sought “smoking gun” for dark matter annihilation [2], as no plausible astrophysical background can produce a diffuse line signature.

The first claims for a spectral feature around 130 GeV were made by Bringmann *et al.* [3] and Weniger [4], who performed a spectral fit to photon events in regions of interest in the inner Galaxy designed to maximize S/N. They found a line structure at 130 GeV with  $4.6\sigma$  significance, or  $3.2\sigma$  after the trials factor correction [4] (for previous studies see [5–8]). This claim was quickly followed up and disputed by a number of groups [9, 10]. Subsequent work by Su & Finkbeiner approached the problem with template fitting, which takes into account the spatial distribution of events along with spectral information, and found  $6.6\sigma$  ( $5.1\sigma$  after the trials factor correction) for an Einasto profile centered  $1.5^\circ$  west of the Galactic center, and also suggested that there may be two lines, at about 111 and 129 GeV. The lower energy line is tantalizing because it matches the expected energy of a  $Z\gamma$  line if the higher energy is the  $\gamma\gamma$  line. These findings have inspired a number of models and further analysis of the *Fermi* data [11–36].

The Earth’s atmosphere provides a convenient source of photons for systematics tests. The continual cosmic-ray cascades in the Earth’s atmosphere produce gamma rays with  $dN/dE \sim E^{-2.8}$  [37]. Because these so-called ‘Earth limb photons’ result from atmospheric cascades, they are produced by interactions in a highly boosted frame, and cannot contain line emission.

In the following, we review the current observational status, estimate the additional exposure needed, and propose a strategy to obtain it while mitigating impact on other science objectives.

## II. CURRENT STATUS OF SIGNAL AND SYSTEMATICS

Although the evidence for a 130 GeV line is compelling, significant concerns about the Galactic center signature remain, including: (1) its statistical robustness, and (2) its possi-

ble cause by an instrumental systematic. We will briefly summarize the current situation, concentrating on statistical properties of the Galactic center excess and – as arguably the most worrisome indication for a systematic – a feature in the low incidence angle Earth limb data.

### A. Time evolution of the signal significance

The first claims of a spectral feature [3, 4] were based on 3.5 years of LAT data (through 4 February 2012). More recent data provide an opportunity to confirm the signal and see how it evolves with time. Because the signal is based on approximately 1 signal count per month, Poisson fluctuations cause the significance to accumulate in something akin to a random walk. The mean trend in significance builds with the square root of exposure ( $\mathcal{E}$ ) but with large uncertainties. A confirmation at  $3\sigma$  of the signal in the original ROI (i.e. no trials factor) would be persuasive, but the exposure required to get an expected significance of  $3\sigma$  is quite different from the exposure required to achieve  $3\sigma$  *with a probability of 95%*.

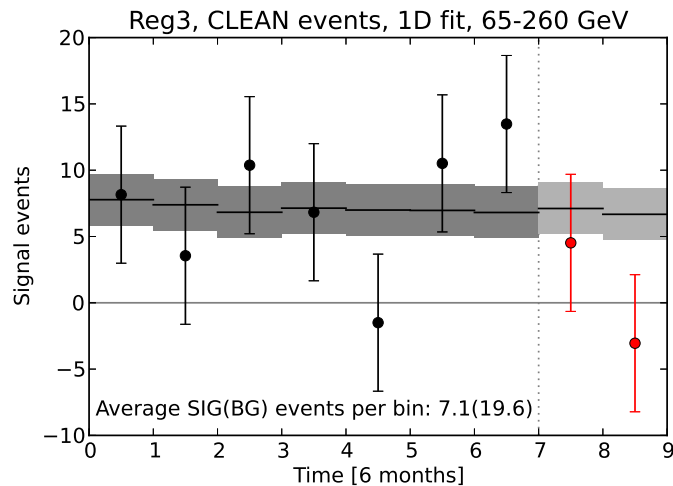


FIG. 1. Number of signal events in 6-month bins starting from 4 August 2008, obtained by an unbinned likelihood fit to the data in Region 3 of Ref. [4]. The gray band shows the expected signal rate with  $\pm 1\sigma$  uncertainty as extracted from data taken until 4 February 2012. In red we show data taken since 4 February 2012 together with the projected event rate.

*Status.* We use the first 3.5 years of data, 4 August 2008 through 4 February 2012, to define the spectral and spatial properties of our signal hypothesis (this is the data set that

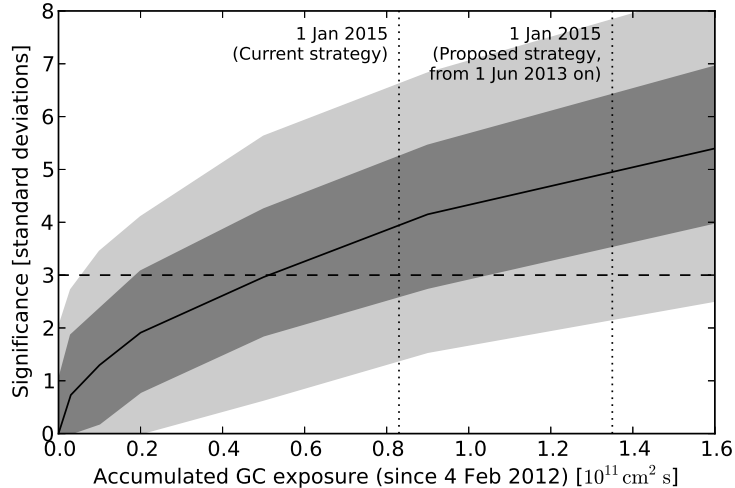


FIG. 2. Expected evolution of signal significance in Region 3 from Ref. [4], starting on 4 February 2012, as function of accumulated exposure. The shaded bands show 68% and 95% CL uncertainties as derived from a Monte Carlo simulation. The assumed signal rate is  $1.2 \pm 0.3$  events per month, the effective background is 3.3 events per month (the values measured prior to 4 February 2012). The first and second vertical dotted lines indicate how much exposure is expected to be accumulated until end of 2014 if the observation strategy remains unchanged, and respectively when the observation strategy proposed in this document is adopted starting from June 2013. Note that without changing the survey strategy, until the end of the three year extension Aug 2016, the accumulated exposure will be  $1.29 \times 10^{11} \text{ cm}^2 \text{ s}$ .

was used in the initial publication, Ref. [3]). Data taken after the 4 February 2012 can then be used to confirm or reject this hypothesis without trials. To be conservative, we will not use the template regression technique from Ref. [38], but follow [3, 4] and use spectral fits in ROIs with large expected S/N. For definiteness, we will only use ‘Region 3’ from Ref. [4], which is one of the regions where the excess was first identified. Below we propose a geometrically similar but much simpler region that we advocate as an alternative for future studies.

We derive the number of excess events  $N_s$  by a maximum likelihood fit to the first 3.5 years of data from Region 3 (using a power-law plus line model). In the fit, we adopt an energy range from 65 to 260 GeV, fix the line position at  $E_\gamma = 129.8 \text{ GeV}$ , and use P7CLEAN events only.<sup>1</sup> We find a number of  $N_s = 50.0 \pm 13.3$  excess events, with a

<sup>1</sup> The details of the fit are identical what was done in Ref. [4], but we checked that similar results are

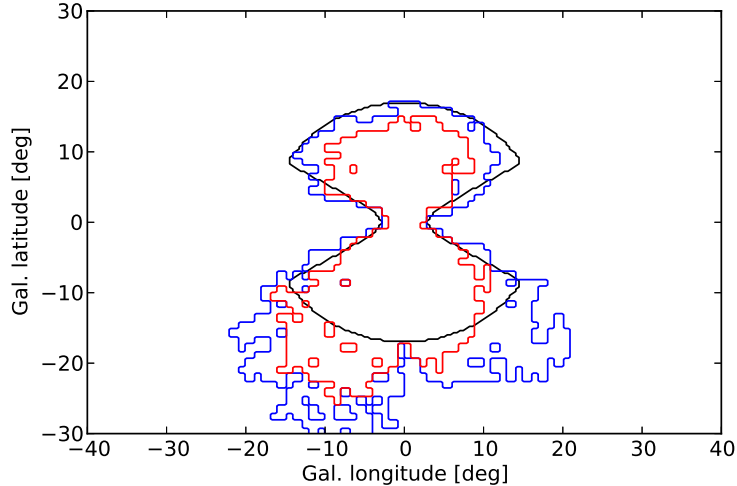


FIG. 3. Region 3 (blue) and Region 4 (red) used in Ref. [4], together with the simpler hourglass region proposed for future studies (cp. also with Fig. 3 in Ref. [1]).

statistical significance of  $s = 4.3\sigma$ . The effective number of background events can be estimated as  $N_b = N_s^2/s^2$ , and is  $N_b = 137.4$ . These parameters together with the details of the fit define our *signal hypothesis*; the *null hypothesis* is that the flux is compatible with a single power law, i.e.  $N_s = 0$ .

In Fig. 1 we show the distribution of these excess events in bins of six months. The first seven bins correspond to the 3.5 years that define the excess, the two red data points are data taken afterwards. Error bars include background fluctuations and are given by  $\Delta N_s = \sqrt{N_s + N_b}$ . To obtain  $N_s$  and  $N_b$ , we fit the data of each six-month bin individually. The gray bands show the number of signal events expected from the above fit to the 3.5 years data, with small variations related to the exposure.

The last two bins are compatible with both the null-hypothesis at the one sigma level, and with the signal-hypothesis at the two sigma level (see also Ref. [39]). In the case of a real signal, the last bin would represent a decent downward fluctuation. However, it would be premature to draw strong conclusions from this single bin.

*Projection.* Going forward, the signal hypothesis predicts that the significance will build as  $\sqrt{\text{exposure}}$ , but with large uncertainties. It is essential to estimate these uncertainties, because we need to know how much exposure is required to *cleanly* separate the signal from the null hypothesis.

---

obtained using Region 4, P7SOURCE events, or a ‘2D’ fit that takes into account incidence angle as well as energy information in the modeling of the line.

In Fig. 2 we show 68% and 95% CL bands for the projected evolution of the signal significance as function of exposure accumulated after 4 February 2012. To generate the plot, we simulate events from a power-law plus line model and derive the signal significance for each realization as described above. The background and signal correspond to the best-fit values obtained in Region 3 with data until 4 February 2012. For different realizations we allow the signal normalization to vary following a normal distribution that is matched to the  $\pm 1\sigma$  flux uncertainties from the 3.5 year results.<sup>2</sup>

The first vertical dashed line indicates the exposure that will be acquired by 1 Jan 2015 with the current survey strategy (in the first 3.5 years, an exposure of  $10^{11} \text{ cm}^2 \text{ s}$  was collected at the GC at 100 GeV). It is likely that a true signal would be confirmed with  $> 3\sigma$  significance, although this is not guaranteed due to the 95% CL error bands that range down to significances of only  $1\sigma$ . Worse, it will be difficult to robustly rule out the signal hypothesis at the  $3\sigma$  level unless the accumulated significance is close to zero.<sup>3</sup> This drives home the point that, left unchanged, the current survey strategy may well leave us with ambiguous results well into 2015. As we will discuss in the next section, a change in the observation strategy will allow a much quicker confirmation/rejection of the signal hypothesis.

*Alternative ROI.* For future analysis of the 130 GeV feature in the LAT data, instead of using the difficult to manage regions from Ref. [4], we propose to use the region shown in black in Fig. 3. This region is (1) geometrically simple and easy to reproduce, and (2) it is centered on the part of the sky where the excess was largest in the previous data. Though we avoid any statement about particular dark matter profiles, it is an *a priori* region for data taken since 4 February 2012. We defined this ROI in  $(\ell, b)$  space as the intersection of  $\ell^2 + b^2 \leq r^2$  and  $\ell^2 \leq (b \tan \varphi)^2 + d^2$ , with  $(r, d, \varphi) = (20^\circ, 3^\circ, 60^\circ)$ .

## B. The Earth limb feature

The most direct indication for an instrumental cause of the Galactic center feature is an excess of 130 GeV photons in low incidence angle events from the Earth limb [38, 40–42]. Although it is challenging to understand how such a feature could possibly be mapped onto

<sup>2</sup> We checked that similar results for the projection evolution are obtained for Region 4, in the hourglass region discussed below, or using the analytical estimates from Ref. [39].

<sup>3</sup> To exclude the signal hypothesis at, say, the  $2\sigma$  level at a specific point in time, the actually observed significance has to lie outside of the predicted 95% CL band in Fig. 2.

the Galactic center while being absent in other test regions, this feature has raised serious concerns about the energy reconstruction of the LAT around 130 GeV. Additional limb data would determine whether the Earth limb feature is indeed a true systematic effect or merely a statistical fluke in light of a large number of trials. If it is a reproducible systematic, additional data may be required to diagnose the software or hardware problem responsible.

We define here the Earth limb excess by selecting P7CLEAN events until 5 Sep 2012 at zenith angles  $Z > 100^\circ$ , incidence angles  $\theta < 60^\circ$ , and excluding events within  $20^\circ$  of the Galactic center. In this data set, the line feature at 130 GeV has a significance of  $2.7\sigma$  when fit in the range 65–260 GeV (for details of the assumed line shape, etc., see Ref. [40]).<sup>4</sup> Data accumulated after 5 Sep 2012 can now be used to test whether this excess is spurious. Using the above cuts, we find that the rate of events above 100 GeV between the start of the mission and 5 Sep 2012 is 9.5 ph/month (in total 474), whereas 36.7 ph/month accumulated between 5 Sep 2012 and 16 Apr 2013. The reason for this increase is the commencement of weekly dedicated limb observations as well as two extended target of opportunity observations in that time period. If the accumulation of low incidence angle Earth limb data continues at this pace, 2.3 years of fresh data will be enough to regenerate the putative limb signature with  $4.0\sigma$  significance on average, or to rule it out with reasonably high significance if it is a fluke. Without a change of the observation strategy, this amount of data would be available end of 2014. As we will discuss next, a change of the observation strategy would help to collect the same amount of low incidence angle Earth limb data in a much shorter time period, and the additional data would be invaluable for diagnosing instrumental problems.

### III. A NEW OBSERVATION STRATEGY

Since the start of the mission, Fermi has spent over 95% of the time in *standard survey mode*. In this mode, the LAT points north of zenith towards the orbital pole by an angle  $Z_{\text{rock}}$  on one orbit, and south of zenith by the same angle on the next orbit; the LAT pointing is confined to the plane perpendicular to its orbital velocity. This observation profile, combined with the precession of the orbit every  $\sim 53.4$  days, allows the LAT to observe the whole sky with approximately uniform coverage. The standard survey mode is only occasionally

---

<sup>4</sup> If we take into account data until 16 Apr 2013, the significance of the Earth limb feature is  $3.0\sigma$ , which is marginally larger.

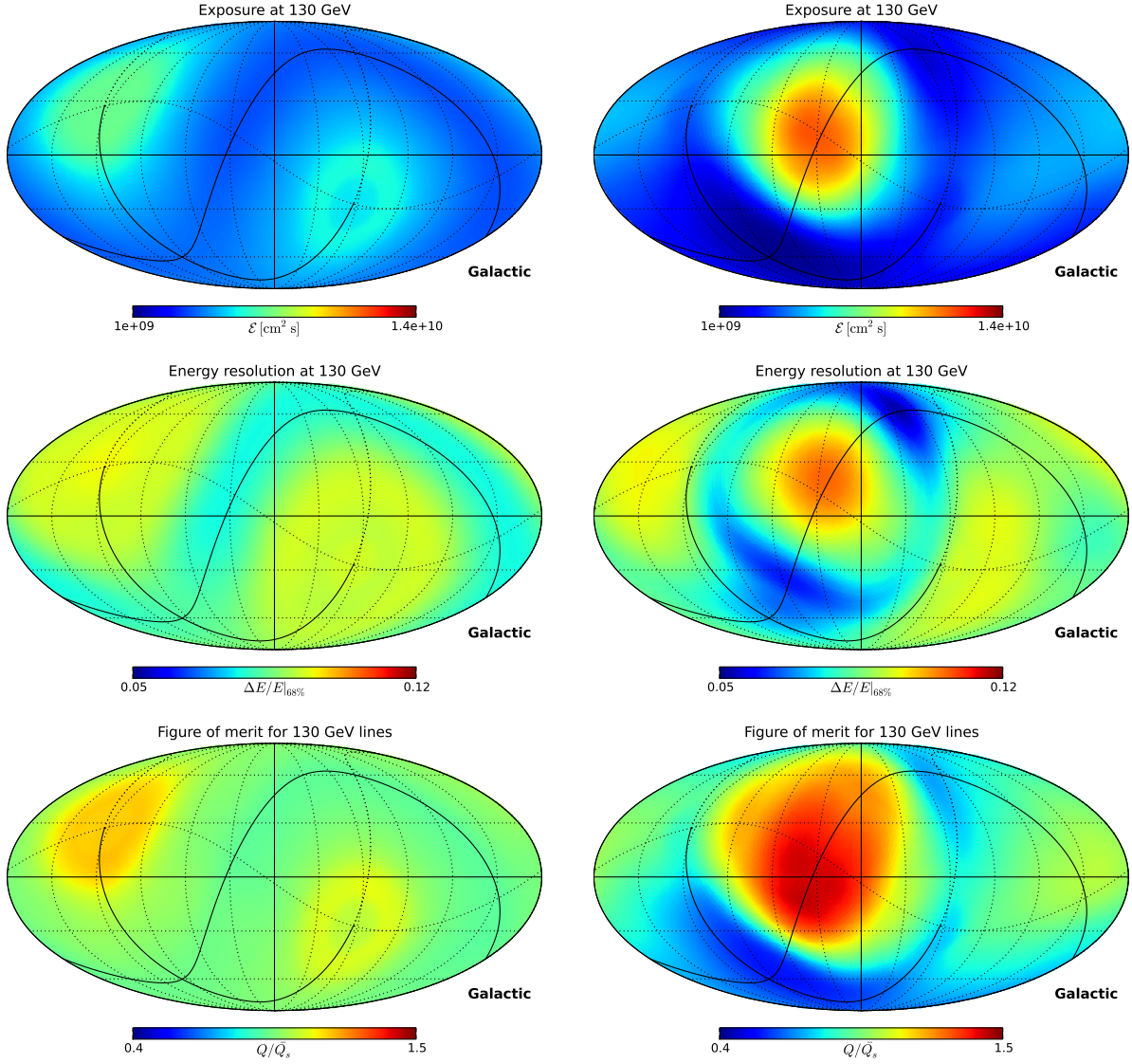


FIG. 4. Evaluation of standard survey mode (*left panels*) and mixed observation strategy (*right panels*). Sky maps are in galactic coordinates ( $\ell$  increases to the left) and averaged over a orbital precession period of 55 days. *Top panels*: Exposure maps in  $\text{cm}^2 \text{s}$ . *Central panels*: Effective energy resolution (half 68% containment width) *Bottom panels*: Figure of merit for gamma-ray line searches. In all panels the overlaid lines show the main axes of the equatorial coordinate system; sky maps are symmetric around the celestial equator.

interrupted for pointed observations of targets of opportunity (ToOs). During such times the LAT may point at a larger zenith angle than usual, even at the horizon. In addition, survey mode is occasionally interrupted by Autonomous Repoints of the observatory for



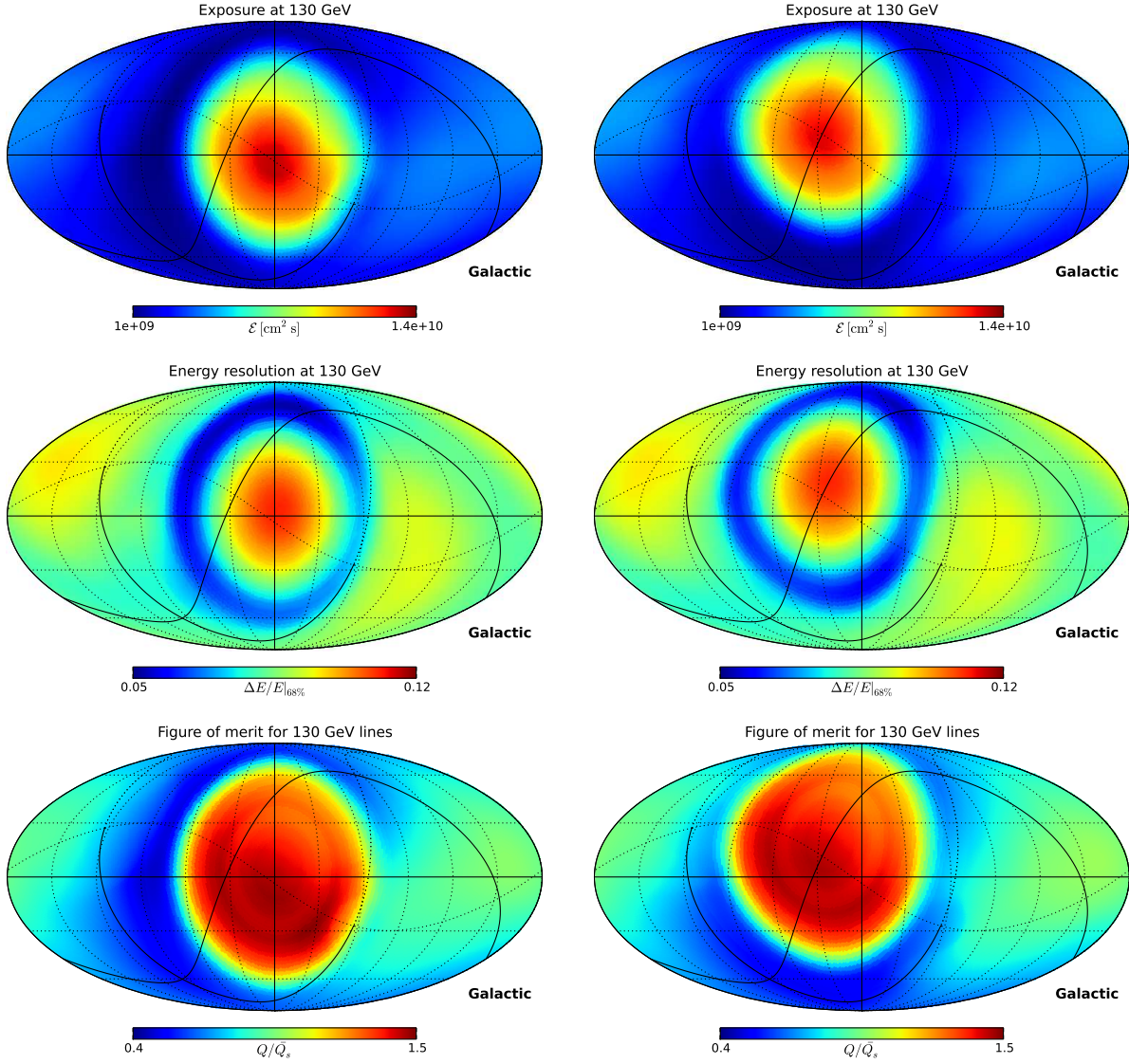


FIG. 5. Same as Fig. 4, but for ‘option1v2’ and ‘option2v2’.

triggered gamma-ray burst follow-up observations, and for calibration.

However, Fermi is capable of very flexible survey mode patterns. For example, a single orbit may include both survey mode and pointed observations (“mixed mode”), increasing coverage of certain parts of the sky. We will explore the impact of such a strategy on the study of the 130 GeV feature at the Galactic center. We focus here on the mixed modes ‘option1v2’, ‘option2v2’ and ‘option3v3’ put forth for discussion by the Fermi mission.<sup>5</sup>

Our goal is to increase the exposure on the Galactic center. The basic strategy would be to switch to pointed observation of the Galactic center when possible, and to follow the

<sup>5</sup> See [http://fermi.gsfc.nasa.gov/ssc/proposals/alt\\_obs/obs\\_modes.html](http://fermi.gsfc.nasa.gov/ssc/proposals/alt_obs/obs_modes.html).

standard survey mode otherwise. More precisely, *Fermi* would slew from survey mode to the target once the target is  $10^\circ$  from Earth occultation, and slew back to survey mode position once the target reenters  $10^\circ$  from Earth occultation. The the Earth Avoidance Angle (EAA) is set to  $30^\circ$ , to avoid the loss of too much exposure during the transition periods. This means that the LAT will track the target only to within  $30^\circ$  of the Earth limb and then hold steady before it switches back to survey mode.

To reduce potential systematics, it is advisable to avoid pointing directly at the target. Instead, it is useful to observe it with a broad distribution of incidence angles. The three mixed modes option1v2, option2v2 and option3v3 differ mainly in what target position exactly is adopted. In option1v2 and option2v2, the position is fixed at (RA, Dec)=( $261.4^\circ$ ,  $-28.9^\circ$ ) and (RA, Dec)=( $261.4^\circ$ ,  $0^\circ$ ), respectively.<sup>6</sup> In option3v3 the target position RA is set to  $261.4^\circ$ , while the target declination varies within the range Dec= $\pm 25.6^\circ$  during one orbital precession period such that the target position remains close to the orbital equator. These variations of the target position yield an improved sky uniformity on short time scales.

#### A. Impact on line searches at the Galactic center

The upper panels of Fig. 4 show exposure maps after 55 days survey mode (left) and mixed mode option3v3 (right) in galactic coordinates. In the mixed mode, the point of highest exposure is at (RA, Dec) $\simeq$  ( $261.4^\circ$ ,  $0^\circ$ ). At the Galactic center, the exposure increases by a factor of 2.23 relative to normal survey mode.

In mixed mode, regions close to the Galactic center are predominantly observed at low incidence angles in the range  $\theta \simeq 5^\circ$ – $50^\circ$  (see Fig. 6). This has impact on the effective energy resolution, which is shown in the central panels of Fig. 4. In direction of the Galactic center the energy resolution is in fact slightly worsen with respect to the standard survey mode ( $\Delta E/E = 9.59\%$  for option3v3 instead of  $\Delta E/E = 8.75\%$ ). However, this loss of resolution has only a small effect on line searches.

In Fig. 5, we show the same information, but for the mixed modes option1v2 (left) and option2v2 (right). The Galactic center exposure increases by a factor 3.0 and 2.5, respectively, whereas the effective energy resolution is 11.1% and 10.0%. Apart from the characteristics at the Galactic center, these modes mainly differ in the impact on other

---

<sup>6</sup> The Galactic center is at RA= $266.4^\circ$ , Dec= $-28.9^\circ$ .

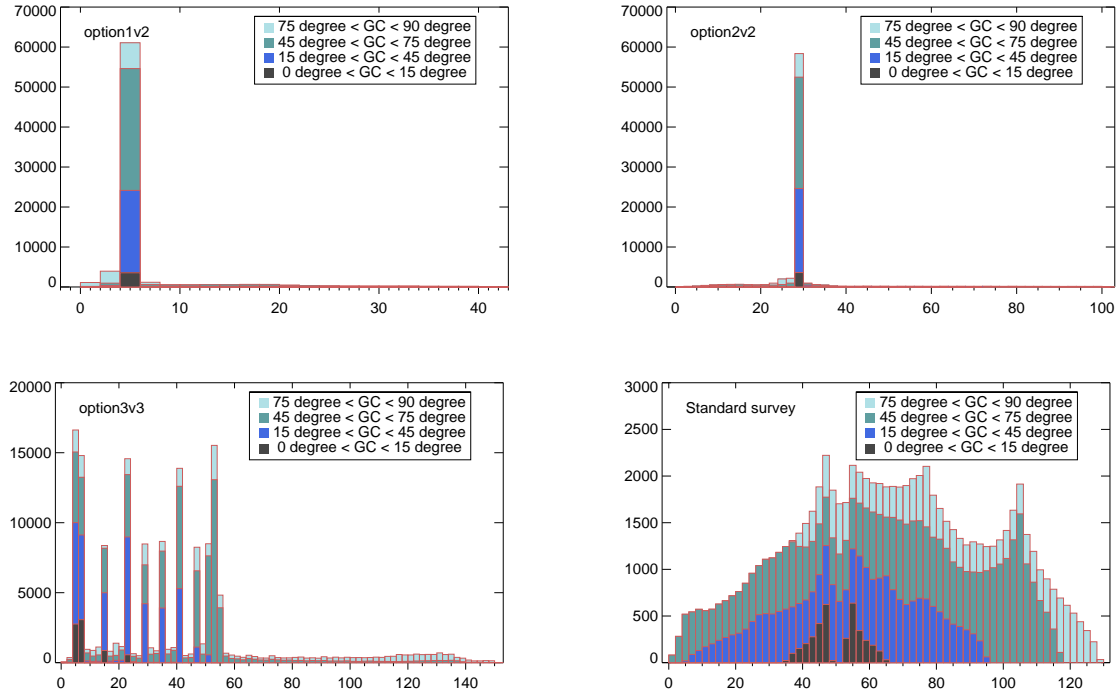


FIG. 6. The distribution of Galactic center theta angle. Each entry in the histogram corresponds to a 30 seconds interval. The colors correspond to the zenith angle of the Galactic center. The plots take account of time spent in the SAA.

science goals, as we will discuss below.

As a convenient *figure of merit* for line searches we define the dimensionless quantity

$$Q \equiv a\sqrt{\mathcal{E}/\Delta E},$$

which is proportional to the expected median line significance in units of standard deviations. Here,  $\mathcal{E}$  is the exposure in  $\text{cm}^2\text{s}$ ,  $\Delta E$  the energy resolution, and  $a$  normalizes  $Q$  such that the spatial mean in survey mode is  $\bar{Q} = 1$ . In the bottom panels of Fig. 4 and 5 we show sky maps for  $Q$  in mixed and survey mode. At the Galactic center,  $Q$  increases by a factor 1.43 when switching to mixed mode option3v3, which would increase the growth rate of the signal significance by 43%, equivalent to doubling the exposure/time.

## B. Impact on Earth limb observations

In general, to keep systematics that might be related to specific incidence angles  $\theta$  under control, it is useful if the Galactic center is observed at a broad distribution of different

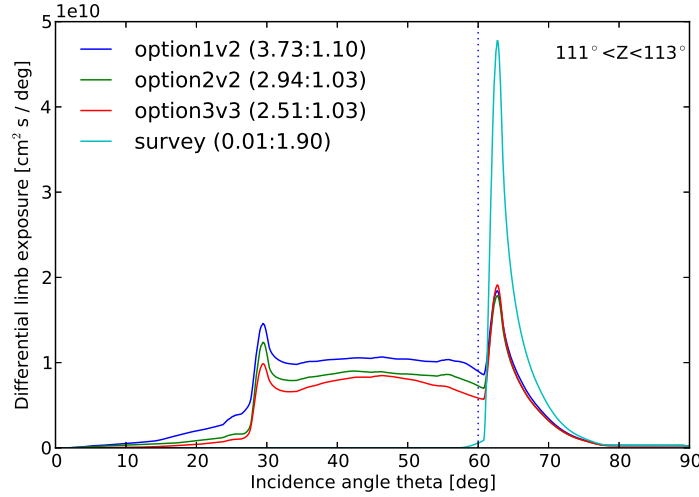


FIG. 7. Differential exposure of Earth limb region (zenith angles  $111^\circ < Z < 113^\circ$ ) as function of incidence angle  $\theta$ . In standard survey mode, incidence angles below  $\theta < 60^\circ$  are not exposed to the Earth limb. However, in mixed observation modes, a large number of Earth limb events would be collected down to incidence angles  $\theta \simeq 30^\circ$ . In brackets we show the exposure below and above  $\theta = 60^\circ$  in units of  $10^{11} \text{ cm}^2 \text{ s}$ .

incidence angles. For the four observation modes, this distribution is shown in Fig. 6. In case of option3v3,  $\theta$  spans a range from  $5^\circ$  to  $50^\circ$  (the discrete distribution comes from jumps in the target position as it follows  $\text{Dec} \simeq 0^\circ$ ). This is a significant advantage when compared to option1v2 and option2v2, which feature pronounced peaks at  $\theta \sim 5^\circ$  and  $\theta \sim 30^\circ$ , respectively.

An important side effect of the mixed mode is the accumulation of additional Earth limb data at low incidence angles, which can be used for checks of instrumental systematics. This happens during the transitions between pointed observation and survey mode. The target comes close to the horizon, while the satellite maintains a minimal distance of  $30^\circ$  from the Earth limb. Consequently, the Earth limb is observed at incidence angles  $\theta \gtrsim 30^\circ$  twice every orbit (1.5 hours).

In Fig. 7, we show the expected differential exposure of the Earth limb at zenith angles  $111^\circ < Z < 113^\circ$ . In standard survey mode, practically no limb data is collected at  $\theta \lesssim 60^\circ$ . However, during mixed mode a very significant number of the detected Earth limb events would be collected at lower incidence angles. This would accelerate the accumulation of low incidence angle Earth limb data with respect to the previous 4.5 years by about a factor of

Mode	Mean exposure [ $10^9 \text{ cm}^2 \text{ s}$ ]	GC exposure [ $10^9 \text{ cm}^2 \text{ s}$ ]
survey	4.74	4.33
option1v2	4.38	13.1
option2v2	4.44	10.7
option3v3	4.56	9.67

TABLE I. Mean exposure (averaged over full sky) and exposure of Galactic center for different observation profiles in comparison. We assume P7CLEAN events at 100 GeV and 55 days of observation.

*five*, and will allow a rapid rejection or confirmation of the 130 GeV feature in part of the Earth limb spectrum. Note that a collection of Earth limb events at incidence angles even lower than  $30^\circ$  is possible if the EAA is set appropriately, however at the cost of losing more exposure on the rest of the sky.

### C. Impact on other science

Changing from survey mode to mixed mode observation will necessarily drag exposure from some parts of the sky towards the Galactic center. In order not lower the scientific power of Fermi, it is imperative that the *integrated* exposure over the whole sky remain as high as possible. Furthermore, for the observation of transient phenomena, it is vital that all parts of the sky are sufficiently covered at least each day; ‘blind spots’ should be avoided.

In Table I, we compare for the four reference strategies the mean sky exposure obtained after 55 days of observation. The overall loss in sky exposure w.r.t. to the standard survey mode is small and between 4% (option3v3) to 8% (option1v2).

The variations of the exposure over different regions of the sky are illustrated in in Fig. 8, where we show a histogram of the distribution of exposure in different sky pixels (using a Healpix projection with  $N = 128$ ). In the case of standard survey mode, the exposure distribution spans a factor of two (being largest at  $\text{Dec}=\pm 90^\circ$ ), whereas it spans a factor 10 in the mixed mode option3v3. However, in no region of the sky does the exposure drop by more than a factor of three relative to normal survey mode.

For transient phenomena, the daily sky exposure is of importance. In Fig. 9 we show for each individual day of the precession period which fraction of the sky is covered by

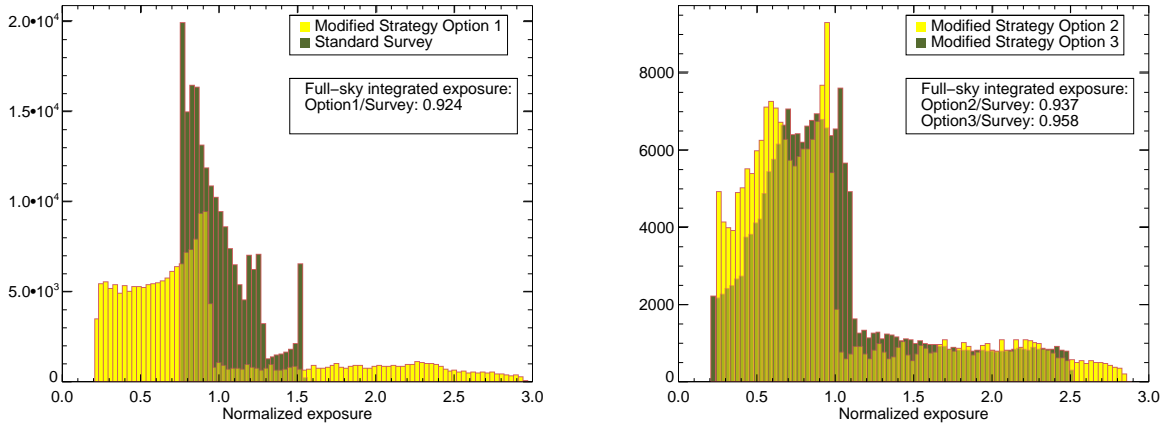


FIG. 8. Histogram of exposure per sky pixel, normalized to standard survey strategy. Left panel compares the mixed mode option1v2 to the standard survey strategy, and the right panel shows the modified strategy option2v2 and option2v3.

Mode	> 150% exposure	< 50% exposure	50% < exposure < 150%
option1v2	25 (12%)	59 (27%)	131 (61%)
option2v2	32 (15%)	45 (21%)	138 (64%)
option3v3	29 (13%)	30 (14%)	156 (73%)

TABLE II. Number (fraction) of transient sources corresponding to different expected exposure given three modified survey strategy. The fraction of expected exposure is compared to the standard survey strategy.

what fraction of the mean exposure. In case of the mixed mode observations option2v2 and option3v3, in less than 5% of the sky the daily coverage drops below 20% of the daily mean, whereas in  $> 80\%$  the coverage remains above 50% of the mean.

The Fermi All-sky Variability Analysis has detected a total of 215 flaring gamma-ray sources over the entire sky based on weekly time intervals of 47 months LAT data [43]. In Fig. 10 we show how the exposure of different variable source types could be affected by changing from survey to mixed mode observations. For the different source classes, we show the fraction of sources that would lose in exposure by than 50% (red), which would gain more than 50% in exposure (green), and which remain relatively unaffected (black). For option1v2, we have 25 sources that would receive more than 150% exposure compared to the standard survey strategy with finer sampling on time domain (including the recently detected Nova

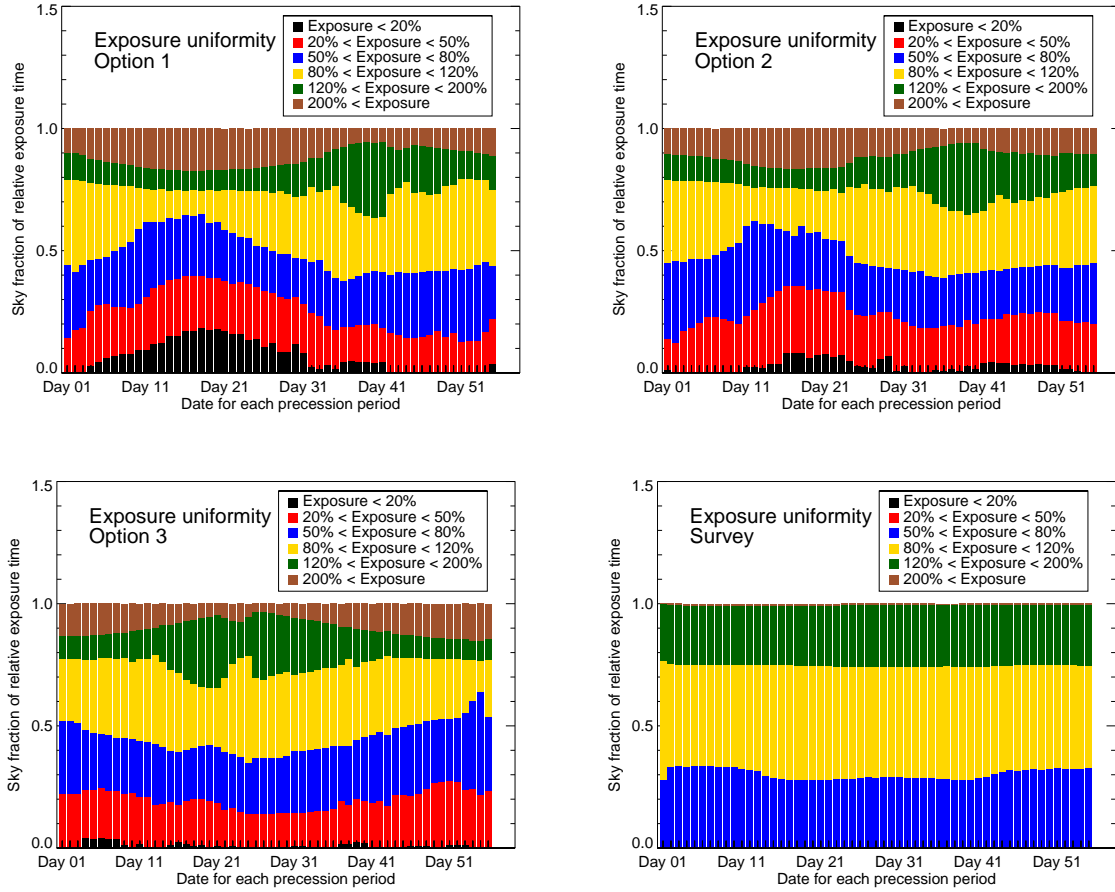


FIG. 9. Daily sky coverage with different range of exposure time normalized to the mean value of the exposure map of each day (in total 55 days to complete on orbit precession period).

Sco 2012), although with the price that 59 sources would receive less than 50% exposure. We note that 61% of the transient sources (131 in total) would receive comparable (50-150%) exposure time for option1v2 and the standard survey mode. In Table II, we compare for the three modified strategies the fraction of transient sources that would obtain  $> 150\%$  exposure,  $< 50\%$  exposure, and  $50 - 150\%$ . As we see from the Table, option3v3 provides a comparable number of sources with  $> 150\%$  exposure, but 50% (33%) smaller sample of sources with  $< 50\%$  exposure for option1v2 (option2v2).

For transient searches on different time scales, both short-term flares on time scales of a few hours and long-term flux variations of a few months, the changed survey strategy would provide the opportunity for a sample of sources with better sampling in the time domain and higher sensitivity of flare detection.

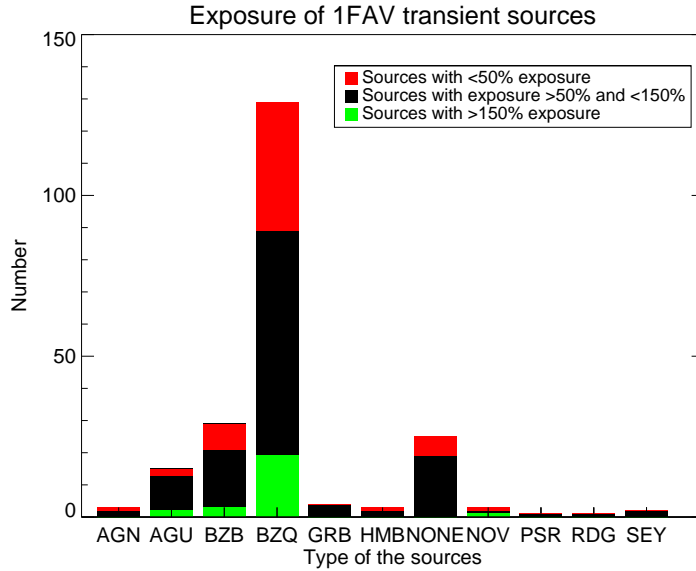


FIG. 10. Source type distribution for the 1FAV catalog [43]. We classify the sources into three categories: sources with expected exposure time (assuming option1v2) less than 50% of the standard survey strategy; sources with expected exposure between 50% to 150% compared to the standard survey strategy; and sources with expected exposure more than 150%.

#### D. Possible triggers

We advocate the change to a new survey strategy as soon as technically feasible. A more conservative approach might involve waiting for certain triggers before initiating a change. For example, one might want to wait until the Pass 8 processing is finished before making a decision. However, it will probably not be public for another year or more, and it is difficult to tie the decision to an internal release; in order for the community to provide input, the decision should be made based upon public data.

Another trigger might be to just wait until a certain significance against/in favour of the signal hypothesis is achieved. However, this could cause a long-enough delay to make a later change inefficient. It would make more sense to make the change immediately, and then have a trigger to revert to normal survey mode when the signal hypothesis is ruled out at some level.



#### IV. DISCUSSION AND CONCLUSION

In this document we have argued for a change in the Fermi survey strategy to increase exposure in the inner Galaxy, and confirm or rule out claims of a 130 GeV spectral line. The principal reasons for a change are:

- *It is important: discovery of a dark matter annihilation line in the Galactic center would be Fermi's greatest accomplishment.* The nature of dark matter is one of the greatest mysteries in physics and astrophysics, and the discovery of a line would be a major step forward for both fields. Exploring the nature of dark matter is one of the major goals of the Fermi project, and a discovery would define Fermi's legacy.
- *Fermi can do it: a modified survey strategy can obtain a decisive measurement, while the status quo may not.* The significance of a line evolves as  $\sqrt{\text{exposure}}$ , but with large uncertainty due to Poisson fluctuations. For example, if the signal hypothesis is correct, the expected signal significance by 1 Jan 2015 is about  $4\sigma$  (Fig. 2). Poisson fluctuations broaden this range such that the actual significance achieved is between  $2.5$  and  $5\sigma$  68% of the time, and between  $1.5$  and  $6.5\sigma$  95% of the time. A clear separation of the signal hypothesis from the null hypothesis requires more data than one might think. If the project continues with standard survey mode until 2016, there is a fair chance that we leave this question unresolved. We cannot permit this to happen.
- *This is a win-win: the proposed change is not bad for other science.* There will be winners and losers in any change, but more time on the inner Galaxy is good for lots of projects (better time coverage for pulsars and transients, etc.). Many wide-angle surveys (SDSS, Pan-STARRs, etc.) have found it fruitful to dedicate a significant fraction of observing time to “deep fields” where greater sensitivity and improved cadence extend the range of phenomena observable. Furthermore, roughly half the sky has more exposure under the new strategy, and even the underexposed regions are still observed on a regular basis for continued monitoring of transients (Fig. 9).

For all of these reasons, we advocate a change in the survey strategy, as soon as possible. For reasons discussed above, ‘option3v3’ put forward by the Fermi mission seems to be the best way to go.

At least for the next several years, Fermi is uniquely able to address the 130 GeV line (with possible competition from HESS-II [44]). If it is an artifact, it is a subtle one – and understanding its origin is important for the dark matter search in particular, and the mission as a whole. If the line is real, we would forever regret missing this opportunity to pursue it aggressively.

- 
- [1] T. Bringmann and C. Weniger, *Phys.Dark Univ.* **1**, 194 (2012), arXiv:1208.5481 [hep-ph].
  - [2] L. Bergstrom and H. Snellman, *Phys.Rev.* **D37**, 3737 (1988).
  - [3] T. Bringmann, X. Huang, A. Ibarra, S. Vogl, and C. Weniger, *JCAP* **1207**, 054 (2012), arXiv:1203.1312 [hep-ph].
  - [4] C. Weniger, *JCAP* **1208**, 007 (2012), arXiv:1204.2797 [hep-ph].
  - [5] A. R. Pullen, R.-R. Chary, and M. Kamionkowski, *Phys.Rev.* **D76**, 063006 (2007), arXiv:astro-ph/0610295 [astro-ph].
  - [6] A. Abdo, M. Ackermann, M. Ajello, W. Atwood, L. Baldini, *et al.*, *Phys.Rev.Lett.* **104**, 091302 (2010), arXiv:1001.4836 [astro-ph.HE].
  - [7] G. Vertongen and C. Weniger, *JCAP* **1105**, 027 (2011), arXiv:1101.2610 [hep-ph].
  - [8] M. Ackermann *et al.* (LAT Collaboration), *Phys.Rev.* **D86**, 022002 (2012), arXiv:1205.2739 [astro-ph.HE].
  - [9] E. Tempel, A. Hektor, and M. Raidal, (2012), arXiv:1205.1045 [hep-ph].
  - [10] A. Boyarsky, D. Malyshev, and O. Ruchayskiy, (2012), arXiv:1205.4700 [astro-ph.HE].
  - [11] E. Dudas, Y. Mambrini, S. Pokorski, and A. Romagnoni, *JHEP* **1210**, 123 (2012), arXiv:1205.1520 [hep-ph].
  - [12] K.-Y. Choi and O. Seto, *Phys.Rev.* **D86**, 043515 (2012), arXiv:1205.3276 [hep-ph].
  - [13] B. Kyae and J.-C. Park, *Phys.Lett.* **B718**, 1425 (2013), arXiv:1205.4151 [hep-ph].
  - [14] H. M. Lee, M. Park, and W.-I. Park, *Phys.Rev.* **D86**, 103502 (2012), arXiv:1205.4675 [hep-ph].
  - [15] A. Rajaraman, T. M. Tait, and D. Whiteson, *JCAP* **1209**, 003 (2012), arXiv:1205.4723 [hep-ph].
  - [16] B. S. Acharya, G. Kane, P. Kumar, R. Lu, and B. Zheng, *ArXiv e-prints* (2012), arXiv:1205.5789 [hep-ph].
  - [17] M. Garny, A. Ibarra, and D. Tran, *JCAP* **1208**, 025 (2012), arXiv:1205.6783 [hep-ph].
  - [18] M. R. Buckley and D. Hooper, *Phys.Rev.* **D86**, 043524 (2012), arXiv:1205.6811 [hep-ph].
  - [19] X. Chu, T. Hambye, T. Scarna, and M. H. Tytgat, *Phys.Rev.* **D86**, 083521 (2012), arXiv:1206.2279 [hep-ph].
  - [20] Z. Kang, T. Li, J. Li, and Y. Liu, *ArXiv e-prints* (2012), arXiv:1206.2863 [hep-ph].

- [21] W. Buchmuller and M. Garny, JCAP **1208**, 035 (2012), arXiv:1206.7056 [hep-ph].
- [22] L. Bergstrom, Phys.Rev. **D86**, 103514 (2012), arXiv:1208.6082 [hep-ph].
- [23] J. H. Heo and C. Kim, Phys.Rev. **D87**, 013007 (2013), arXiv:1207.1341 [astro-ph.HE].
- [24] J.-C. Park and S. C. Park, Phys.Lett. **B718**, 1401 (2013), arXiv:1207.4981 [hep-ph].
- [25] S. Tulin, H.-B. Yu, and K. M. Zurek, Phys.Rev. **D87**, 036011 (2013), arXiv:1208.0009 [hep-ph].
- [26] M. Asano, T. Bringmann, G. Sigl, and M. Vollmann, (2012), arXiv:1211.6739 [hep-ph].
- [27] J. M. Cline, Phys.Rev. **D86**, 015016 (2012), arXiv:1205.2688 [hep-ph].
- [28] N. Weiner and I. Yavin, Phys.Rev. **D86**, 075021 (2012), arXiv:1206.2910 [hep-ph].
- [29] N. Weiner and I. Yavin, Phys.Rev. **D87**, 023523 (2013), arXiv:1209.1093 [hep-ph].
- [30] J. Fan and M. Reece, ArXiv e-prints (2012), arXiv:1209.1097 [hep-ph].
- [31] X.-Y. Huang, Q. Yuan, P.-F. Yin, X.-J. Bi, and X.-L. Chen, JCAP **1211**, 048 (2012), arXiv:1208.0267 [astro-ph.HE].
- [32] D. Whiteson, JCAP **1211**, 008 (2012), arXiv:1208.3677 [astro-ph.HE].
- [33] I. Cholis, M. Tavakoli, and P. Ullio, Phys.Rev. **D86**, 083525 (2012), arXiv:1207.1468 [hep-ph].
- [34] K. Rao and D. Whiteson, JCAP **1303**, 035 (2013), arXiv:1210.4934 [astro-ph.HE].
- [35] D. Whiteson, (2013), arXiv:1302.0427 [astro-ph.HE].
- [36] E. Carlson, T. Linden, S. Profumo, and C. Weniger, (2013), arXiv:1304.5524 [astro-ph.HE].
- [37] A. Abdo *et al.*, Phys.Rev. **D80**, 122004 (2009), arXiv:0912.1868 [astro-ph.HE].
- [38] M. Su and D. P. Finkbeiner, ArXiv e-prints (2012), arXiv:1206.1616 [astro-ph.HE].
- [39] C. Weniger, (2013), arXiv:1303.1798 [astro-ph.HE].
- [40] D. P. Finkbeiner, M. Su, and C. Weniger, JCAP **1301**, 029 (2013), arXiv:1209.4562 [astro-ph.HE].
- [41] A. Hektor, M. Raidal, and E. Tempel, (2012), arXiv:1209.4548 [astro-ph.HE].
- [42] E. Bloom, E. Charles, E. Izaguirre, A. Snyder, A. Albert, B. Winer, Z. Yang, and R. Essig, ArXiv e-prints (2013), arXiv:1303.2733 [astro-ph.HE].
- [43] 1229445, (2013), arXiv:1304.6082 [astro-ph.HE].
- [44] L. Bergstrom, G. Bertone, J. Conrad, C. Farnier, and C. Weniger, JCAP **1211**, 025 (2012), arXiv:1207.6773 [hep-ph].